

Solar Activity Monitoring Through Real Time Recording of VLF Wave Amplitude

A.S.Rajagopalen, B.K.Darshan, G.Murugan

Abstract— In its latest findings, NASA has come up with a prediction of a massive solar storm (flare) that can hit earth anytime in 2012-13. Right from GPS systems, credit card transactions, mobile phone services, communication services, radio and air travel to smart power grids and electrical transformers, all are vulnerable to the solar storm. The damage can be controlled by putting satellites in safe mode. The power grids can be saved by disconnecting them from the supply and transformers. This will require an accurate forecasting about the coming solar storm. This project is designed to monitor solar flares on Earth by tracking changes in Very Low Frequency (VLF) radio transmissions as they bounce off Earth's ionosphere. The strength of the received signal changes according to the extent of ionization in the ionosphere. Thus, by monitoring the amplitude of VLF signals, the appearance of solar flares can be detected.

Index Terms—Radio SkyPipe, Solar Flare, Sound Card, Very Low Frequency

I. INTRODUCTION

A. Overview

The primary driver of the interplanetary space weather affecting earth is the Sun's varying emission of electromagnetic radiation and solar wind plasma which is an ionized gas consisting of protons, electrons, and other heavy particles ejected from the Sun's corona at a mean velocity of 400-500 km/s. Galactic cosmic radiation contributes only 5-10 % of the total radiation, and thus, is not a major driver of weather of the space from the earth's point of view. Near-Earth space weather (i.e., within the Earth-Moon orbital system) is primarily the resultant of the Sun's electromagnetic radiation and plasma interactions with the Earth's intrinsic geomagnetic field. The variability in the weather of the space is closely tied to the 27 day rotation period of the Sun and the Sun's approximate 11-year sunspot cycle. During solar maximum (i.e., time of maximum sunspot activity and associated solar flare eruptions), the magnitude value of the variability can become very large, producing highly hazardous space environmental conditions

B. Solar Flares and its cause of occurrence

A solar flare is a sudden energy release in the solar atmosphere from which electromagnetic radiation, energetic particles and bulk plasma are emitted. It is a sudden brightening in an active region usually near a complex group of sunspots of the photosphere.

Solar flares are thought to be a result of intense, abrupt release of solar magnetic energy by magnetic reconnection.

A large number of high-energy electrons are accelerated during the course, which generate intense X-ray and radio bursts. Plasmas are heated to several to tens of millions of degrees in the corona to emit soft X-rays as well.

A great magnitude of plasma from the surface of the sun is released outwards. When this plasma returns back to the surface of the sun, it collides with denser material in the chromosphere (the second uppermost layer of the sun between the photosphere and the corona). This interaction ejects great quantities of energy in the form of electromagnetic radiation, known as solar flares and coronal mass ejections. These are carried by solar wind out into space, and are sometimes directed toward the earth based on the location of the sunspot from which the flare erupted

C. Impact of solar flares on earth

There are two main industries on earth impacted by solar flares: communication and power industry. Solar events cause great problems for the communications industry. Influx of solar plasma and electromagnetic radiation into the near-earth space environment can cause the Earth's magnetosphere to go into geomagnetic storming conditions. Geomagnetic storms have the capacity to severely degrade the radio wave propagation characteristics of the ionosphere, resulting in complete damage and black-out of communications, radar, and navigation, and harm the electronics on satellites and in antennas. The amount of radio waves absorbed increases, resulting in radio blackouts. GPS systems, credit card transactions, mobile phone services, and air travel are also disrupted. The power industry has difficulties with solar flares as well, as their transformers can possibly become jammed. Solar flares create extra electrical currents (millions of Amperes strong) when its charged particles become electromagnetically coupled to earth's magnetic field. The electrical grid functions as an antenna, allowing these currents to flow into transmission lines. This would saturate transformers, which start to overheat, and their insulation breaks down.

Common satellite anomalies induced by space weather include computer processing errors, loss of contact with satellite, shut-down of satellite, and disorientation of the satellite due to the radiation and energetic particle import on star navigation sensors.

Manuscript published on 30 October 2013.

* Correspondence Author (s)

A.S.Rajagopalen*, Completed B.E from Velammal Engineering College, Anna University, Chennai, India.

B.K.Darshan Completed B.E from Velammal Engineering College, Anna University, Chennai, India.

G.Murugan, Completed B.E from Velammal Engineering College, Anna University, Chennai, India.

© The Authors. Published by Blue Eyes Intelligence Engineering and Sciences Publication (BEIESP). This is an [open access](http://creativecommons.org/licenses/by-nc-nd/4.0/) article under the CC-BY-NC-ND license <http://creativecommons.org/licenses/by-nc-nd/4.0/>

Satellite orbits can easily decay due to satellite drag resulting from space weather induced higher atmospheric density.

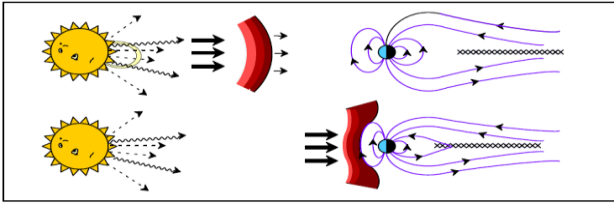


Fig : Solar Flares Distort Earth's Magnetic Field, Causing Geomagnetic Storms

D . Basic principle of operation

VLF signals are transmitted by VLF stations for navigation and positioning purposes, communication with submarines, or as a time measuring standard. These signals are reflected by the D-region of the ionosphere. The electron concentration and the altitude of the lower edge of the ionosphere change when solar flares occur. The change in the waveguide characteristics affects the propagation parameters of VLF signals. Since the amplitude and phase of VLF signals are stable under undisturbed solar conditions, the appearance of X-ray flares can be detected by the perturbation of the signal phase delay and amplitude, in an indirect way

II. PROPAGATION OF VLF RADIO WAVES

The characteristics of the lower boundary of the Earth-ionosphere waveguide are determined by electrical conductivity of soil and water surface. The upper boundary of the Earth-ionosphere waveguide changes its characteristics with diurnal and seasonal variations of lower ionosphere. These changes are predictable, so may be considered as regular. The unpredictable changes occur when abrupt change of electron concentration in the D region takes place and therefore the reflection coefficient changes at locations containing the wave reflection points. One of the causes that affect the waveguide upper boundary is the ionization by a solar X-ray flare. The change of waveguide upper boundary caused by a solar X-ray burst, can be manifested in two main ways:

a) Sharpness of the boundary of the D region due to an increase of electron concentration simultaneously with a descent of the boundary. The reflection of "mirror" type occurs, and the propagation calculations can be carried out in the same way as if the boundary surface had metal characteristics. The dissipation of wave energy is negligible, even smaller than in the unperturbed propagation conditions. The effect of such disturbance of the D region is a rise of the received VLF signal amplitude to the maximum, then decreasing to unperturbed value, following the magnitude of the solar X-ray irradiance.

b) Increase of electron content in the entire D region, without sharpness of the boundary. The wave penetrates into the D region, up to the altitude at which the wave frequency matches the plasma frequency of the medium and where the reflection takes place. Along the ray path inside the D region, so called "deviative" absorption from point to point is present and wave energy is dissipated at each step. The result is a drop of the received VLF signal amplitude to the minimum followed by a rise to unperturbed value, corresponding to the end of the solar flare X-ray burst.

In both cases a) and b) , the phase delay follows the variation of the amplitude, but the changes are not necessarily of the same sign.

A. Calculation of Amplitude and Phase of VLF Signals

The estimation of amplitude and phase of VLF signals can be done using software called LWPCv21 (Long Wavelength Propagation Capability). The input parameters to the software are as follows.

- Latitude and Longitude of transmitter station
- Azimuth angle
- Inclination angle and strength of magnetic field
- Ground conductivity and relative dielectric constant
- Slope of conductivity vs. height
- Reference height of ionosphere

III. CLASSIFICATION OF SOLAR FLARES

Flares are classified based on the magnitude of peak burst intensity of X-ray irradiance (I_x), measured in 0.1 – 0.8 nm wavelength band

Table : Classification of Solar Flares Based on X-Ray Irradiance

Class	X-Ray Irradiance
B-Class	$<10^{-6}$ W/m ²
C-Class	10^{-6} - 10^{-5} W/m ²
M-Class	10^{-5} - 10^{-4} W/m ²
X-Class	$>10^{-4}$ W/m ²

Each class has 9 subdivisions, ranging from 1-9. Example: M6 = 6×10^{-5} W/m². The effects of solar flares on the ionosphere depend on the X-ray irradiance, and the duration of the flare

A. Variation of VLF Signal Parameters

The typical example of VLF signal amplitude and phase delay diurnal change observed on a quiet summer day is given below. The X-ray irradiance, I_x , did not exceed magnitude of 10^{-6} W/m², namely, no significant flare events occurred. When the X-ray irradiance intensity is less than 10^{-6} W/m², no significant changes in amplitude or phase are observed. The amplitude is lesser during the day because of absorption by the increased electron concentration in the ionosphere during daytime. The phase follows the variation of the amplitude, but not necessarily of the same sign (because phase depends on constructive or destructive interference between sky waves and ground waves).

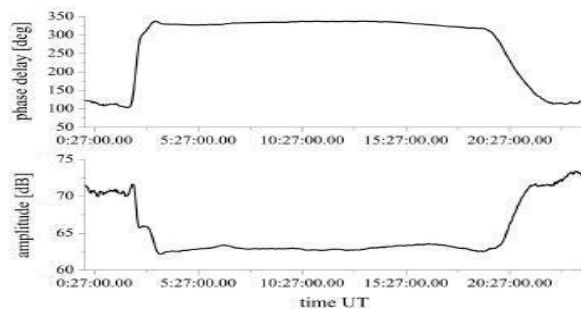


Fig : Diurnal variation of amplitude and phase of VLF signals on an unperturbed day

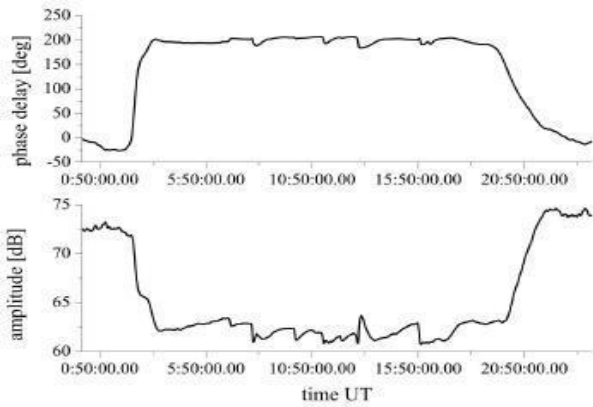


Fig : Diurnal Variation of Amplitude and Phase of VLF Signals on a disturbed day

B. C1-C3 class solar flares

The simultaneous monitoring of VLF signal amplitude and X-ray irradiance during a moderate C-class flare is shown below.

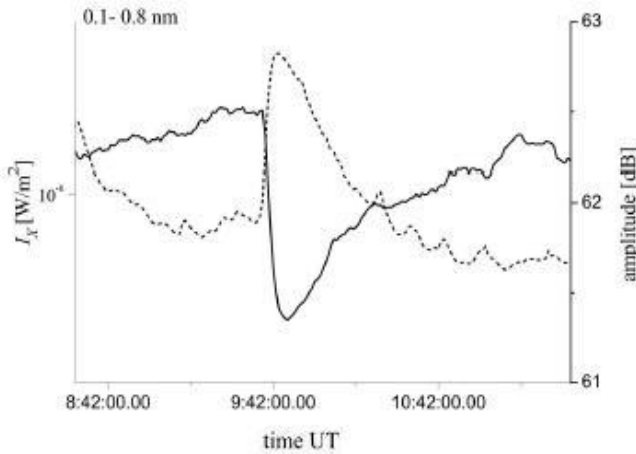


Fig : C1 – C3 class flares

There is a rapid decrease of amplitude to a minimum and a much slower recovery to its value preceding the flare. The minimum amplitude value is time delayed by a few minutes with respect to the X-ray peak irradiance due to the sluggishness of the ionosphere in reaching the peak electron concentration. This is caused due to the recombination process. The difference between the extreme amplitude value and the value of amplitude at the moment corresponding to the extreme value, but on the nearest undisturbed day, ΔA is upto -2 dB. The VLF signal penetrates deep into the D region due to lower ionization, thus the ray path is longer. The amplitude decreases due to deviative absorption of wave energyscale,

C. C4-C4 class flares

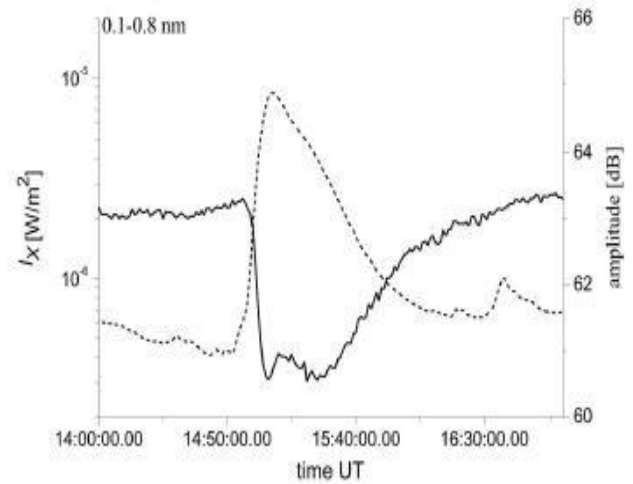


Fig: C4 – C9 class flares

The amplitude decreases, but the decrease terminates before the X-ray irradiance reaches the peak value. After the first minimum, the amplitude oscillates, and reaches a second minimum few minutes after the peak of the X-ray irradiance. After that, the amplitude slowly recovers to its value before the flare. In this case, ΔA is upto -3 Db

D. M1-M4 class flares

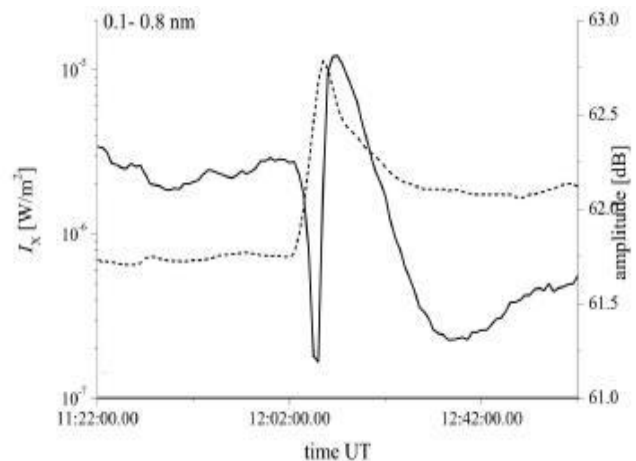


Fig : M1 – M4 class flares

The amplitude peak between the first and the second minima rises above the level of the undisturbed amplitude value. This peak is followed by a decrease, below the level of the undisturbed amplitude. ΔA at minima is upto -4 dB. ΔA at maxima is upto 2 dB. The reflection of VLF signals occurs at a sharp boundary of the D region (due to increased electron concentration, and descend of the boundary), without penetration into the region (called mirror reflection). Dissipation of wave energy is negligible, even smaller than in unperturbed conditions. Hence, the amplitude of VLF signals increases above the level of the unperturbed value

E. M5 – M9 class flares

The changes in the amplitude of the VLF signal during the day with respect to the X-ray irradiance is given below

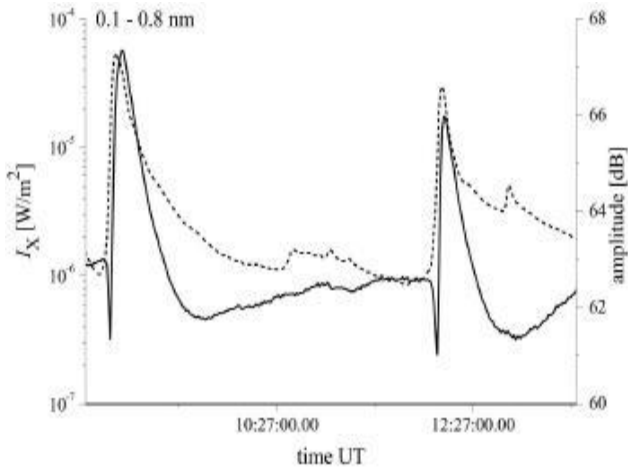


Fig: M5 – M9 class flares

The first amplitude minimum becomes less expressed, when compared with moderate M-class flares. The transition of reflection based on deviative absorption to mirror reflection takes a few minutes. The amplitude minimum is due to deviative absorption, followed by the rise of amplitude to a peak due to mirror reflection. ΔA at minima is upto -2 dB, and ΔA at maxima is upto 5 dB

F. X1 – X9 class flares

These types of flares are very uncommon. This results in very large X-ray irradiance, and correspondingly large peaks in the VLF amplitude chart

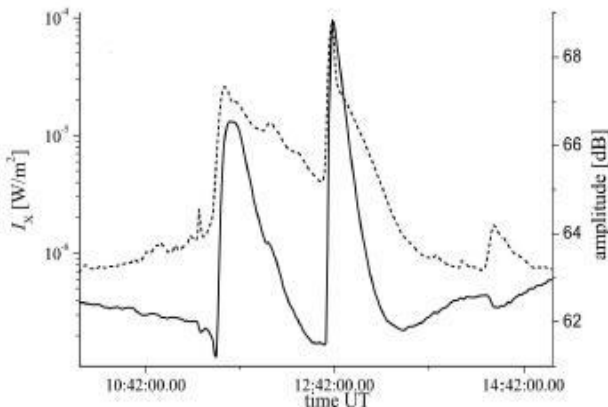


Fig: X1 – X9 class flares

The greater the X-ray peak irradiance, the higher the amplitude peak above the level of the regular diurnal value. ΔA at minima is upto -1 dB, while ΔA at maxima is upto 10 dB

IV. HARDWARE DESCRIPTION

A. Antenna

The antenna shown below is called a wire loop antenna. It is a frame that holds up big loops of wire. As the electromagnetic field from a VLF station passes by the loop, a very small (~0.1 mV) electrical current is induced in the wire. Fundamentally, a loop antenna is an LC (inductor capacitor) circuit which resonates at some frequency. An inductor stores magnetic energy, while a capacitor stores electric energy. The inductance is formed by the wire loop. The capacitance is formed by the wiring metal surface, running in parallel along the loop.

Wire resistance is small, though always present in a wire and increases as the length of the wire increases. Also, when the number of windings increases, the resistance of the wire increases too, causing the amplitude of the signal to drop. However, the resistance is inversely proportional to the thickness of the wire



Fig : Antenna

Specifications

- Length of wire: 120 m
- Diameter of wire: 0.044 inch (1.1176 mm)
- Type of wire: Insulated, Single stranded
- Number of turns: 24-25
- Diameter of pipe: 1 inch (2.54 cm)
- Type of pipe: PVC
- Dimensions of antenna: 1.25 m X 1.25 m

B. Main PCB

The main PCB consists of the following sections:

- Power supply circuit
- Pre-Amplifier
- Frequency board
- Post-Amplifier
- Full wave rectifier
- Audio circuit
- DATAQ Circuit



Fig : Main PCB

a) Power Supply Circuit

The Power Supply Section takes input from the 9-10 V, 200 mA transformer and produces both regulated positive and negative 5 V supplies. The fuse (F1) is a re-settable 250 mA circuit breaker. The AC to DC voltage conversion is achieved by a half-wave rectifier (diodes D1 and D2) and smoothed by capacitors C1 and C2 (Higher frequencies bypassed by C5 and C6). The DC working voltage on these caps should be rated at two times the input voltage, plus we added 50% more as a precaution, therefore: $WVDC = 2.5 \times V_{ac}$ (input voltage) = 25 V DC. The diodes (D3, D4, D5, and D6) prevent a reverse voltage situation that can result when the capacitors are charged up and power reapplied on the input. Caps C3, C4, C7, and C8 are part of the filtering. The two status-LEDs visible on the front panel show independently that both power supplies are functioning. The LED colour assignments are as follows:

- +5 V is green.
- 5 V is yellow

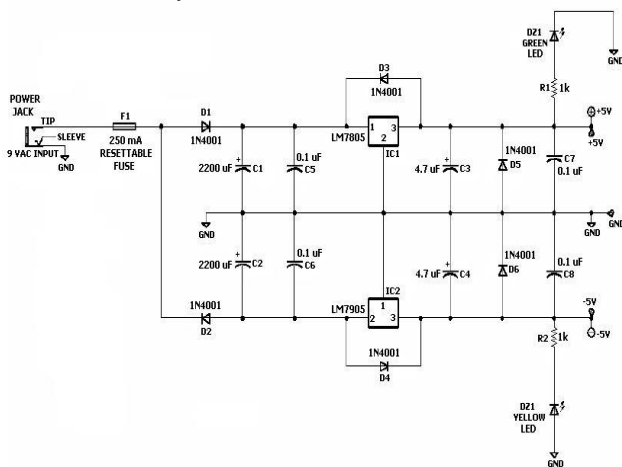


Fig : Power Supply Circuit

b) Pre Amplifier

The antenna input is inputted through a TNC connector. Capacitor C8 isolates DC voltage on the input as well as performs a high-pass filter RC function, consisting of C8 (0.1

μF) and R4 (2.2 k Ω). The cut-off frequency is 723 Hz to help reject 50 Hz power-line hum.

$$f_o = 1 / (2\pi RC) = 1 / (2\pi \times 2.2k\Omega \times 0.1\mu F) = 1 / (2\pi \times 2.2 \times 10^3 \times 0.1 \times 10^{-6})$$

$$f_o = 723 \text{ Hz}$$

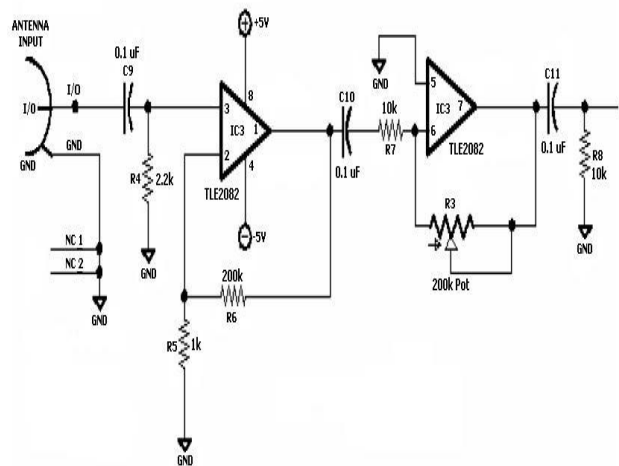


Fig : Pre Amplifier Circuit

The R4 resistor also serves as an AC impedance match to the antenna, however this value cannot be optimized due to the variability of antenna design and consequences to the f_o frequency response of the high-pass filter, thus it is better to make up for the loss in the impedance match by increasing the RF gain. The first stage of the preamp (IC3) is a non-inverted input amplifier with a gain of 201. The output (DC decoupled) runs to the next stage, which is an inverted input amplifier that has a potentiometer (R3) to vary the gain from 0-20, giving a total gain of 0-4,020.

IC3 Non-Inverted input op-amp gain formula ($A = \text{Amplification}$)

$$A = (R5 + R6) / R5 = (1 \text{ k}\Omega + 200 \text{ k}\Omega) / 1 \text{ k}\Omega$$

$$A = 201 \text{ (Fixed gain)}$$

IC3 Inverted input op-amp gain formula

$$A = R3 / R7 = (0 \Omega \text{ to } 200 \text{ k}\Omega) / 10 \text{ k}\Omega$$

$$A = 0 \text{ to } 20 \text{ (Adjustable gain)}$$

c) Frequency Board

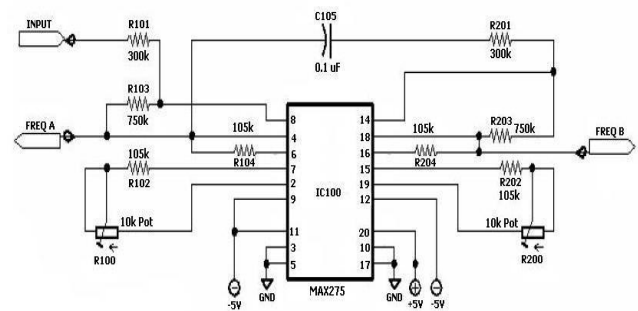


Fig : Frequency Board Circuit

The frequency board has a MAX275 continuous analog filter, configured as a 4-pole Butterworth bandpass filter. There are two filters and 4 resistors are assigned to each filter. Resistors R100 – R104 are for the first filter and R200 – R204 are for the second filter (or stage).



The frequency board is a separate PCB to make it easier to change the center frequency. This board has to be swapped in order to monitor another VLF signal.

The resistors used should be 1 % or better, to ensure that the frequency tuning can be achieved accurately. The two potentiometers R100 and R200 are used to vary the center frequency by a small margin (<100 Hz).

Resistor Calculations

Q value of filter = 170 (Default)
 Bandpass gain, BP_Gain = 2.5 (Default)
 $R2 = R102 + R100 = R202 + R200 = (2 \times 10^9) / f_0 = (2 \times 10^9) / (18.2 \times 10^3)$
 $R2 = 110 \text{ k}\Omega$
 $R102 = R202 = 105 \text{ k}\Omega$ (fixed)
 $R100 = R200 = 0 \text{ to } 10 \text{ k}\Omega$
 $R4 = R104 = R204 = R2 - 5 \text{ k}\Omega = 105 \text{ k}\Omega$
 $R3 = R103 = R203 = (Q \times 2 \times 10^9) / (f_0 \times 25)$
 $= (170 \times 2 \times 10^9) / (18.2 \times 10^3 \times 25)$
 $R3 = 750 \text{ k}\Omega$
 $R1 = R101 = R201 = R3 / BP_Gain = 750 / 2.5 = 300 \text{ k}\Omega$

Table : MAX275 Tuning Resistor Values

Resistor	Value
R100 = R200	10 kΩ Pot
R101 = R201	300 kΩ
R102 = R202	105 kΩ
R103 = R203	750 kΩ
R104 = R204	105 kΩ

Tuning the frequency board

- Connect the main PCB to power supply through a 9V 200mA step down transformer.
- Set the frequency generator output to the smallest output signal possible, and then attenuate the signal further with a simple 2-resistor circuit.
- Connect the TNC connector of coaxial cable to the antenna input in main PCB.
- At the other end of the coaxial cable, connect the leads from the signal generator.
- Connect the ground probe of the oscilloscope to a GND point on the main PCB.
- Use the other oscilloscope probe to probe the test point 'INPUT'. Adjust the RF gain control potentiometer (R3) on the main PCB to attain voltage level of 100 mV peak-to-peak in the oscilloscope.
- Set the frequency of 18.2 kHz in the frequency generator. An error of 100 Hz is fine. The signal generator should not drift off from the set frequency.
- Put the oscilloscope probe on the test point 'FREQ A'.
- Adjust R100 to achieve the peak signal response. Carefully notice the amplitude on the scope while turning the potentiometer in either a clockwise or counter-clockwise direction; one of these directions will cause the signal amplitude to rise. At some point, the amplitude will cross its maximum and begins to fall. Simply reverse the direction of the potentiometer and the signal will again rise back up. Find the setting on the potentiometer that gives the peak response to the input frequency.
- Repeat step 9 for test point 'FREQ B', and adjust potentiometer R200.

k) If a clicking sound is heard coming from the potentiometer while turning, then try reversing directions. If either limit of the potentiometer is reached, and still the peak response is not found, then the frequency to be tuned is not possible with the current resistor values on the frequency board

d) Post Amplifier

This stage is included as a contingency, so as to deal with unknown and variable conditions of a weak signal or poor antenna design. This includes a selector switch (DP3T). Higher gain values are needed to make the input signal audible for antenna orientation. For data logging, minimum gain is required

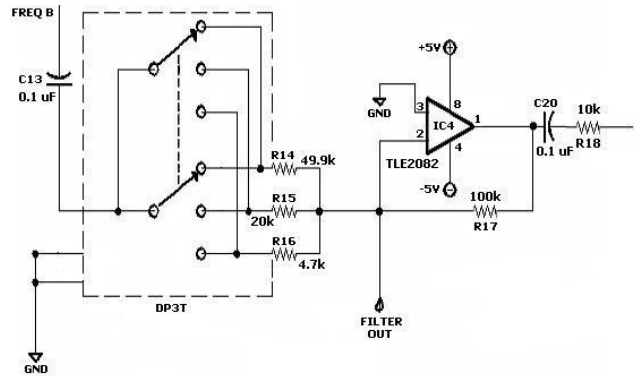


Fig : Post Amplifier Circuit

This stage is included as a contingency, so as to deal with unknown and variable conditions of a weak signal or poor antenna design. This includes a selector switch (DP3T). Higher gain values are needed to make the input signal audible for antenna orientation. For data logging, minimum gain is required.

$A = R17 / R_x$

$A = 100\text{K}\Omega / R_x$; where R_x is one of R14, R15, or R16

Table : Post Amplifier gain settings

Resistor	Value	Gain
R14	49.9 kΩ	2.004
R15	20.0 kΩ	5.000
R16	4.7 kΩ	21.277

e) Full wave rectifier

The audio buffer circuit receives the Test point 'Signal Detect' which is the full-wave, rectified signal. Test point 'Signal Strength' is the integrated signal to produce the signal strength – this is a DC level. The RC circuit (R33 and C21) has an RC time constant is approximately between 5 and 9 seconds. ($T = RC = 20 \text{ k}\Omega \times 470 \text{ }\mu\text{F} = 20 \times 10^3 \times 470 \times 10^{-6}$, $T = 9.4 \text{ s}$). This is approximate because capacitors have lower precision tolerances. R20 is a discharge resistor to provide a small load to discharge the capacitor (C21) in order to make the circuit respond to a lowering level faster than allowing its internal resistance to discharge the capacitor.



The design of this filter is such that it carefully rejects short lived signal bursts, such as lightning, but allows longer persistent signal-strength changes such as those caused by solar flares, to affect the overall signal strength characteristics. Without this filter in place, the resultant graph will be too noisy to reliably detect solar flares, especially smaller class-C flares

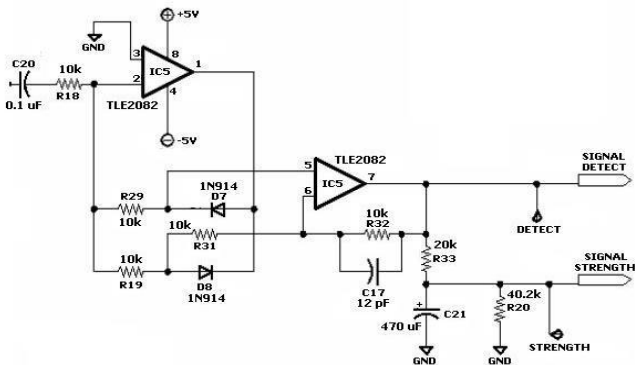


Fig : Full wave rectifier circuit

f) Audio Circuit

IC4 is a unity-gain buffer; C14 isolates the DC component to the line-out level audio output to be connected to amplified speakers. The connector is a stereo connector with the left and right channels connected together

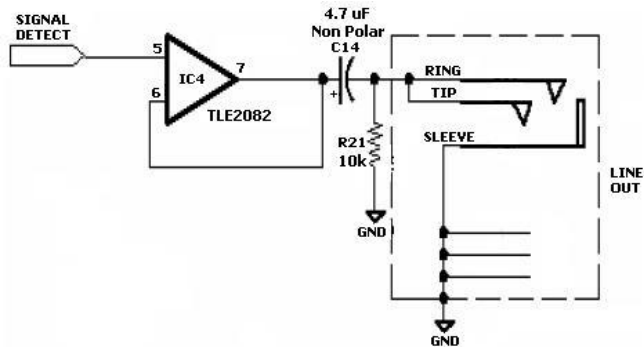


Fig : Audio Circuit

g) DATAQ Circuit

The LT1490 op-amp allows voltages to swing from rail-to-rail. Stage 1 has a gain of 33.127 ($A = R8 / R10 = 267 \text{ k}\Omega / 8.06 \text{ k}\Omega, A = 33.127$). C12 and C13 dampen fluctuations and spikes. C16 stabilizes the voltage on the input to form a stable reference. Stage 2 is a voltage shifter with a gain of 1. The shifter works because the (-) input is tied to +5 V through R11, the inverter input makes the output to go to -5 V, the midpoint between R12 and R11 form a summing point therefore translates the input DC level to -5 V to + 5 V, a 10 V range

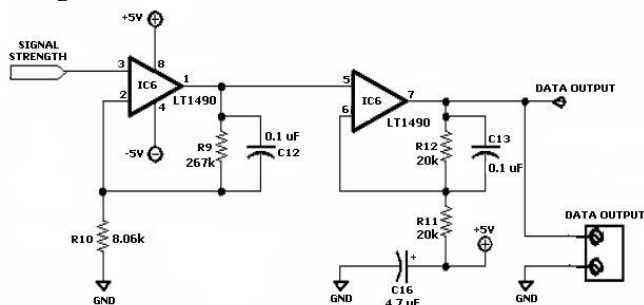


Fig : DATAQ Circuit

C. Components outside the main PCB

a) Audio Amplifier with speaker

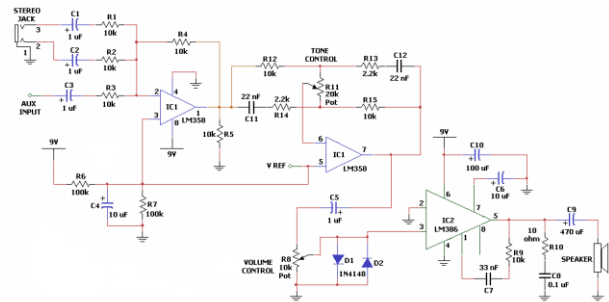


Fig : Audio Amplifier with speaker

Role of the components

- 1 μF capacitor: DC blocking, AC couples the input signal
- 10 k trim pot: voltage-divider for volume control
- 10 μF capacitor: Internal AC bypass
- 10 k Ω resistor and 33 nF capacitor between pins 1-5: bass-boost feedback circuit, helps compensate for the poor low-frequency response of the speaker
- 470 μF capacitor: DC blocking
- 10 Ω resistor and 0.1 μF capacitor: a 'snubber' circuit for high-frequency stabilization, it prevents potential oscillation due to inductive loading.
- Back-to-back diodes at the input terminal of the device: These diodes clamp the input voltage on pin 3 at $\pm 0.7 \text{ V}$, to ensure that excessive voltage is not applied to this pin as it could potentially damage the circuit

b) DC Voltage Chopper

The circuit consists of a 555 Timer, a few op-amps, and a FET that acts as a switch. The 555 timer is used as an oscillator. It generates a square wave of frequency 8.5 kHz. The square wave oscillates between GND and +VCC. R1 charges the capacitor C2 and R2 discharges it.

The frequency of oscillation can be given as follows
 $f = 1/T = 1 / (0.693 \times (R1 + 2R2) \times C2)$
 $= 1.44 / ((1000 + 2 \times 8000) \times 10 \times 10^{-9})$
 $= 8470 \text{ Hz}$

A balanced dual $\pm 12 \text{ V}$ supply is used for 555 timer and IC741 op-amp. The power supply consists of a 15-0-15 500 mA center tapped transformer, a bridge rectifier using four 1N4007 diodes, a positive voltage regulator (L7812), a negative voltage regulator (LM7912), a green LED (for +12 V indication), an yellow LED (for -12 V indication), and a few capacitors. The capacitors are for filtering AC ripples after rectification. The difference between the input and output voltages of the regulator IC is called as dropout voltage. It must be typically 2 V even during the low point on the input ripple voltage, for proper functioning of the regulator

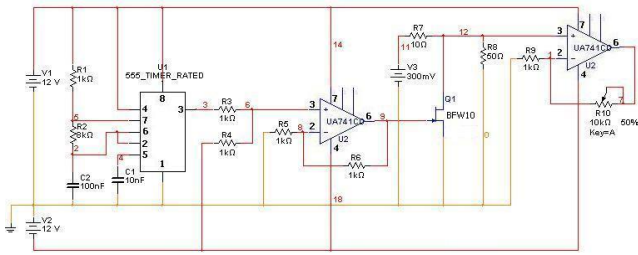


Fig : 555 Timer – FET DC Chopper Circuit

The first IC741 op-amp makes the square wave all negative. It is a non-inverting summer. The output voltage is given by the sum of the voltages at the non-inverting input of the op-amp, since the gain is unity. The square wave now oscillates between GND and $-V_{CC}$. This is applied to the gate of the FET BFW10, which is an n- channel FET. It switches ON when the gate-to-source voltage is below the cut-off voltage (8 V), and switches OFF when it is above the cut-off voltage. When it is ON, the drain-to source voltage is applied to the next stage. Otherwise, the output voltage of the FET is 0. The output voltage from the main PCB is applied across the drain and source of the FET

c) Soundcard

The sound card serves the purpose of an oscilloscope. At its most basic level, an oscilloscope consists of analog to digital converter, set of cables, a software and a display mechanism. The cables are relatively easier to be built. The sound card (also known as motherboard sound chip) converts the voltage to digital data and software can be obtained free, that can display the data on the screen. A three conductor shielded cable with a regular 3.5 mm stereo phono plug will do the job of an oscilloscope cable. The stereo cable plugs into the 'line-in' jack on the sound card (the line-in jack is usually colored blue).

The sound card used for this purpose is an Intex ESS ES1946_1938 PCI AudioDrive (WDM).

V. SOFTWARE DESCRIPTION

A. Radio SkyPipe

Radio-SkyPipe (RSP) is a computer program that is used to collect and display real world data in the form of a strip chart. A strip chart is simply a line graph where the horizontal (X) axis is time and the Y axis represents the value of whatever is being measured. The chart thus is a depiction of how some value changes over time. Perhaps the only thing that makes it different from an ordinary chart is that it is usually used to chart the data in real time, that is, as the data is collected. In the past, strip chart recorders were mechanical devices that scrolled a continuous piece of graph paper under a moving pen.

The data source can be just about anything that can be electronically measured. This could be the temperature, amount of light, battery drain, or the strength of radio noise, etc. Step one is to translate the phenomenon to be measured into an electrical signal that the computer can read. This problem can be addressed in two primary ways. If the signal consists of an electrified sound wave, it is possible to feed the signal into the computer sound card. Sound consists of rapidly changing vibrations. Only this type of signal can be identified by the computer sound card

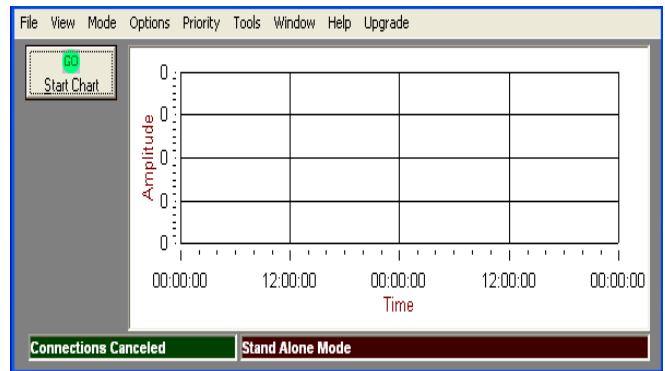


Fig: Radio SkyPipe Interface

B. Soundcard Oscilloscope

This software can be used for the display and analysis of sound waves. The data can be recorded in two ways, either directly from the sound card (with a microphone or LINE input), or from a source such as a CD or Media player. The input to the oscilloscope is defined by the Windows sound mixer. The software obtains its input data for the sound card via the Windows interface. Also the software does not communicate directly with the sound card. Thus any sound card problems should be troubleshoot at the operating system level itself.

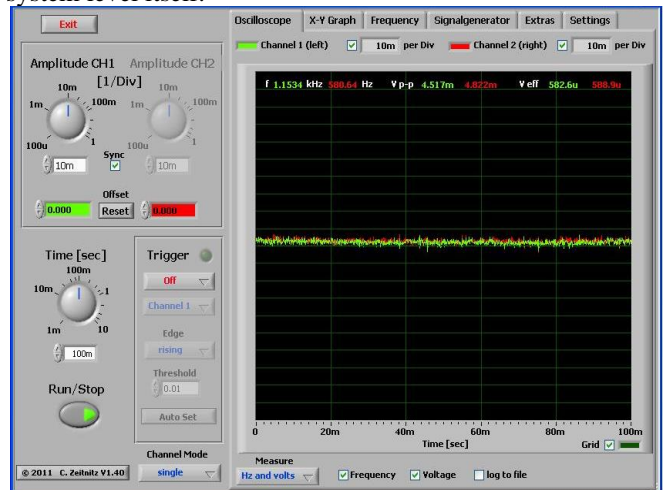


Fig : Soundcard Oscilloscope Interface

VI. METHODOLOGY

The procedure in monitoring solar flares is not very complex, but has to be performed very precisely in order to receive the best possible results. The most difficult part is to find a location for the antenna. The antenna has to be pointing towards the VLF transmitting station (INS Katabomman, Tirunelveli). Also, it has to be placed in a location free from electrical interference, away from power lines and transformers. Once a suitable location is identified, the antenna is placed there. The coaxial cable from the antenna is connected to the main PCB. The audio amplifier with speaker circuit is connected to it as well. The antenna is oriented for maximum sound output from the speaker. The sound should be like white noise.



A good signal will sound like rushing wind. Once the antenna is located and oriented, the recording process shall be initiated.

The DC chopper circuit is connected to the main PCB, and the audio amplifier with speaker circuit is disconnected. The stereo cable from the chopper circuit is plugged into the line-in jack of the sound card. The reception of the signal from the antenna is verified using the Soundcard Scope software. The signal amplitude is recorded as a strip chart in Radio SkyPipe software. The strip chart is then saved with .SPD extension

VII. SIMULATION RESULTS

The solar activity recorded using Radio SkyPipe software as a strip chart on 7th, September 2013 is shown below. Although no major solar events were recorded during the period of observation, the day-night transition in amplitude of the received signal can be clearly noted. The occurrence of solar flares would cause drastic peaks to appear in the VLF signal amplitude vs. time chart. Since no such peaks are visible, it can be assumed that no significant solar flares occurred on that day. The lower amplitude of the signal during the day is due to absorption of wave energy by an increased number of electrons in the ionosphere. The increased electron concentration is attributed to the fact that the sun is more active during the daytime, when compared to the night time.

It needs to be mentioned here that the amplitude of the signal plotted in the strip chart is a relative measurement only. The actual VLF signal amplitude is different from the plotted value. It is not indicative of the intensity of X-ray irradiance from the sun. This is because there are various stages of amplifiers in the intermediate circuitry. The gain of these amplifiers can be varied as per requirement. Also, the mixer settings of the sound card can be varied, and is different for different sound cards.

communication, and several other industries. Thus, it is worthwhile to design a device that can monitor the flares, keeping the costs at the minimum at the same time. Solar Flare Detector is designed specifically with this intention. Overall, this solar flares experiment was of great interest and provided magnificent outcomes that will be of assistance to humanity during times under the presence of solar flares

This detector is inactive during the night, because the influence of solar activity on the strength of VLF signals diminishes after sunset. The remedy would be to install a similar receiver on the other side of the earth (that is facing the sun at the time), and provide a means to transmit the collected data to the locally installed receiver.

The detector falls asleep when the VLF transmitting station is shut down for maintenance. This happens once a week, as per an unpublished schedule. This problem can be overcome if the receiver can be tuned to receive VLF signals from different transmitting stations. For this, the frequency board will have to be replaced, that is tuned to another VLF transmitting station.

REFERENCES

- [1]. D. Grubor, D. Sulic and V. Zigman (2005), 'Influence of Solar X-Ray Flares on the Earth- Ionosphere Waveguide', Serb. Astron., J. No. 171, pp. 29-35.
- [2]. J. Y. Liu, C. H. Lin, H. F. Tsai and Y. A. Liou (2004), 'Ionospheric Solar Flare Effects Monitored by the Ground-Based GPS Receivers: Theory and Observation', Journal of Geophysical Research, Vol. 109.
- [3]. Norm Cohen and Kenneth Davies (1994), 'Radio Wave Propagation'.
- [4]. Qu Ming, Shih Frank, Jing Ju and Wang Haimin (2004), 'Automatic Solar Flare Tracking Using Image Processing Techniques'.
- [5]. Sujay Pal, Tamal Basak and Sandeep. K. Chakrabarti (2010), 'Results of Computing Amplitude and Phase of the VLF Wave using Wave Hop Theory', Advances in Geosciences, Vol. 27.
- [6]. M. Waheed-uz-Zaman and M. A. K. Yousufzai (2011), 'Design and Construction of Very Low Frequency Antenna', Journal of Basic and Applied Sciences, Vol. 7, No. 2, pp. 141-145.

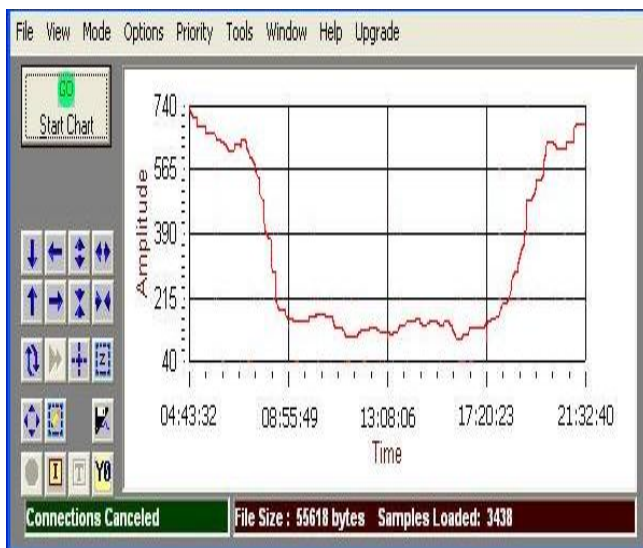


Fig: Recorded VLF Signal Amplitude vs. Time Chart

VIII. CONCLUSION AND FUTURE WORK

From the recorded data, it can be concluded that the project is successful in monitoring solar flares. Solar flares are a rare phenomenon; hence the monitoring of flares is not considered time or cost effective. However, strong flares can cause considerable economic losses to power, radio

